

PACS numbers: 87.64.Dz; 87.53.Wz; 42.62.Be
DOI: 10.1070/QE2002v032n11ABEH002326

Light scattering study of rheumatoid arthritis

J. Beuthan, U. Netz, O. Minet, A.D. Klose, A.H. Hielscher, A. Scheel, J. Henniger, G. Müller

***Abstract*. The distribution of light scattered by finger joints is studied in the near-IR region. It is shown that variations in the optical parameters of the tissue (scattering coefficient μ_s, absorption coefficient μ_a, and anisotropy factor g) depend on the presence of the rheumatoid arthritis (RA). At the first stage, the distribution of scattered light was measured in diaphanoscopic experiments. The convolution of a Gaussian error function with the scattering phase function proved to be a good approximation of the data obtained. Then, a new method was developed for the reconstruction of distribution of optical parameters in the finger cross section. Model tests of the quality of this reconstruction method show good results.**

Keywords: *biomedical functional imaging, near-infrared diaphanoscopy, optical diffusion tomography, rheumatic diseases, scattered light distribution.*

1. Introduction

Rheumatoid arthritis (RA) is the most common inflammatory arthropathy with 1%–2% of the population being affected by this chronic, mostly progressive disease. It often primarily affects small joints, especially finger joints. A small size of joints permits the application of optical transillumination (or diaphanoscopic) methods [1]. Inflammation of joints caused by rheumatic diseases starts with an inflammatory process of capsule synovial structures, called 'synovitis'. Simultaneously, the filtration properties of the synovialis are changed, which leads to a rise in the amount of enzymes within the synovia, resulting in the maintenance of the inflammatory reaction. Later, villous granulation tissue (pannus) develops in the synovialis (Fig. 1), which destroys the cartilage and bone structures [2]. It is obvious that during these first stages, the scattering (μ_s) and absorption (μ_a) coefficients change (Figs 2 and 3) [3].

To perform diaphanoscopy (tomography) experiments, we first measured the optical parameters of tissues at wavelengths 685 nm and 905 nm (Tables 1 and 2) [4]. The results show that a laser diode emitting at 685 nm can

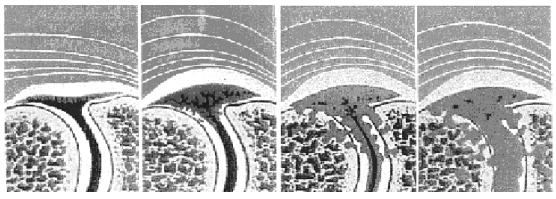

Figure 1. Sketch of the four pathologic stages of rheumatoid arthritis (left to right) [2]: (1) initial stage of synovitis, cell-rich exudat, hyperemia, (2) increase of proliferation of the connective tissue, initial stage of tendinitis, (3) disintegration of the articular cartilage; destruction of bone structures, (4) joint ankylosis, deformation.

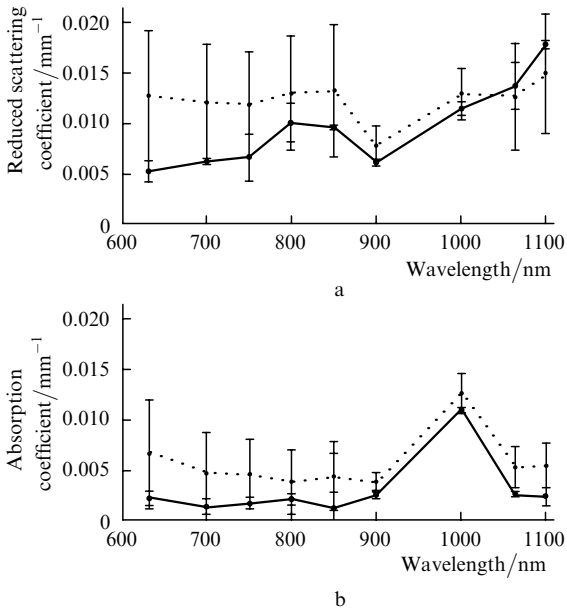

Figure 2. Reduced scattering coefficient (a) and absorption coefficient (b) of synovialis in healthy (solid line) and pathologic (dotted line) states.

J. Beuthan, U. Netz, O. Minet, G. Müller Institute for Medical Physics and Laser Medicine, Free University of Berlin, Germany, Fabeckstrasse 60-62, 14195 Berlin; tel: + +49 30 8449 23 23, fax: + +49 30 8449 23 99, e-mail: j.beuthan@lmtb.de, http://www.medizin.fu-berlin.de/imtpl;
A.D. Klose, A.H. Hielscher Columbia University New York, Dept. of Biomedical Engineering, ET351 Mudd Building, MC 8904, 500 West 120th Street, New York, NY 10027; e-mail: ak2083@columbia.edu, http://www.columbia.edu/~ahh2004;
A. Scheel Department of Medicine, Nephrology and Rheumatology, Georg-August-University, Goettingen, Germany, Robert-Koch-Strasse 40, 37075 Goettingen;
J. Henniger Department of Physics, Technical University Dresden, Germany, 01062 Dresden; e-mail: henniger@physik.tu-dresden.de

Received 12 September 2002
Kvantovaya Elektronika **32** (11) 945–952 (2002)
Submitted in English

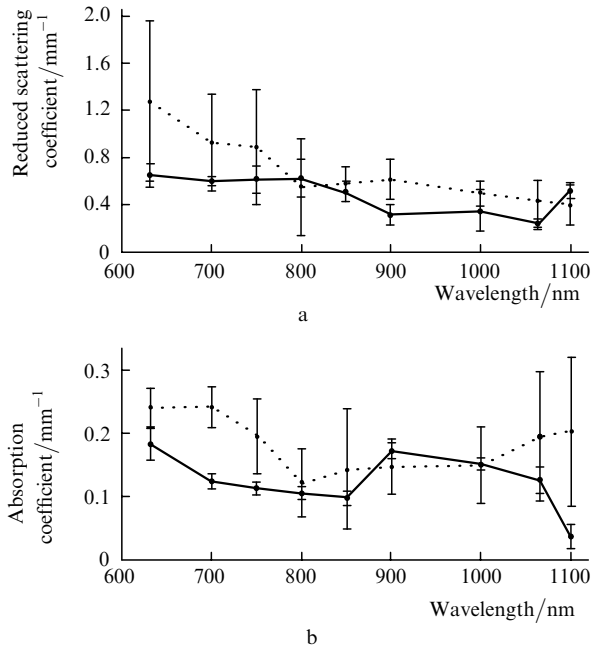

Figure 3. Reduced scattering coefficient (a) and absorption coefficient (b) of synovialis in healthy (solid line) and pathologic (dotted line) states.

be used for diaphanoscopy. The experimental setup for measuring light scattered by finger joints and the results are shown in Figs 4 and 5, respectively. Fig. 5 shows two distributions of light scattered by a healthy finger joint [left hand, curve (*1*)] and by a diseased finger joint [right hand, curve (*2*)], respectively.

A first clinical study by Scheel et al. (2002) showed that laser transillumination of finger joints could be useful as a sensitive follow-up analysis of joint inflammation [5]. Below, we will show that the linear signal transfer theory can be used for a rough but fast approximation of the data.

Table 1. Optical parameters (*ex vivo*) of a healthy finger joint at 685 nm and 905 nm [4] (the data for a diseased joint are given in parantheses).

Tissue	$\lambda = 685$ nm		$\lambda = 905$ nm	
	μ_a/mm^{-1}	μ_s'/mm^{-1}	μ_a/mm^{-1}	μ_s'/mm^{-1}
Skin	0.02	1.95	0.01	1.32
Bone	0.08	2.1	0.08	1.7
Cartilage	0.17	1.8	0.13	1.0
Articular capsule	0.15 (0.24)	0.6 (1.1)	0.17 (0.15)	0.35 (0.62)
Synovia	0.004 (0.011)	0.006 (0.012)	0.005 (0.007)	0.006 (0.008)

Table 2. Assignment of the parameters of the Gaussian distribution to the optical parameters.

Reduced scattering coefficient/cm^{-1}	Absorption coefficient/cm^{-1}	y_0	w	A
5.8	0.4	0.5454	29.89	28.54
11.6	0.4	0.1362	36.26	57.45
23.2	0.4	−0.267	39.07	86.85

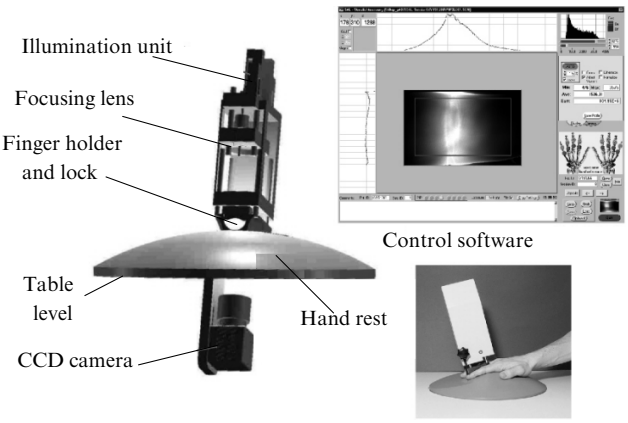

Figure 4. Experimental setup for measuring the distribution of light scattered by finger joints. The system consists of an illumination unit (laser diode array), a camera system, and an ergonomically adapted hand and a finger holder.

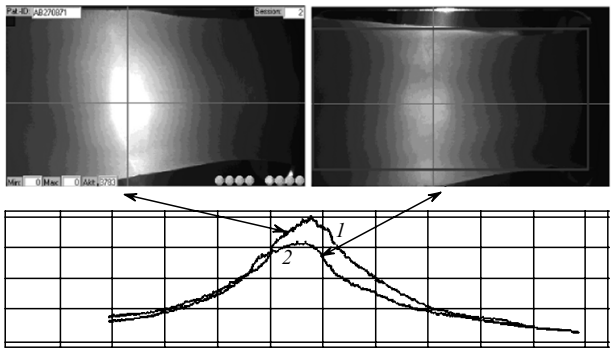

Figure 5. Distributions of light scattered by a healthy (*1*) and an RA diseased (*2*) finger joint.

2. Some aspects of the linear signal transfer theory

The system theory was developed from the combination of the operational calculus of N. Wiener [6] and the transfer theory of K. Kuepfmueller [7]. The system theory is used for the introduction of the optical transfer function. With the introduction of the so-called transfer (or system) function, the question arose how to apply this theory to problems in optical tissue diagnostics. The use of the existing basic transfer (or system) function permits approximated estimates of distributions of light scattered under conditions of a well-defined geometry. This method can be used for RA diagnostics because variations in the optical parameters of the tissue at different stages of the disease change the distribution of scattered light. In this case, measurements and numerical simulations can be performed using a relatively simple phantom set.

According to the transfer theory described below, a formal step should be made within the framework of the measuring geometry. Consider a 'virtual finger joint', representing a slab with the homogeneously distributed optical parameters of the tissue, which are defined as weighted averages of the optical parameters of a real finger joint (see Figs 6a, b).

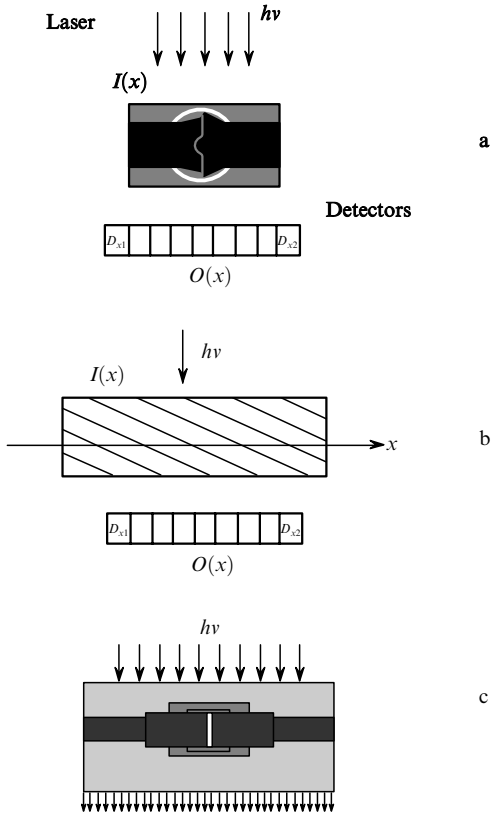

Figure 6. (a) Geometry of the experiment (laser diode array and detectors) with a finger joint. (b) Model of the object representing a 'virtual finger joint' featuring optical parameters that are typical for a real joint, but are homogenously distributed unlike the case (a). (c) Model of a PIP finger joint for direct calculation of light propagation, which consists of five components: bone, capsule, synovialis, synovial fluid, and surrounding tissue (muscle, tendon, skin).

When a finger joint is studied by NIR diaphanoscopy, we can specify a laser spot of a certain geometry, the power density, and the wavelength at the system entry. This 'transfer distribution' is then measured on the opposite side of the finger (in principle: point spread function – since the transfer photons have lost their 'coherence memory' after 10 scattering events, latest), subject to time and position in variance and system linearity by approximation during the measurements.

Considering the scheme in Fig. 6b and applying the operational calculus (including Laplace transformation) according to Wiener, the following equation can be written for a point radiation source and linear detection:

$$\frac{L\{O(x)\}}{L\{I(x)\}} = L\{G(x)\}, \tag{1}$$

where $I(x)$ and $O(x)$ are the light intensity distributions over the coordinate x at the system entrance and exit, respectively, and $L\{G(x)\}$ is the transfer function.

According to Wiener and Kuepfmueller, we introduce the operator p into the Laplace transformation. For simplicity, we will represent the spatial frequency in the form

$$\Omega = \Omega(x). \tag{2}$$

It follows from (1) that

$$O(p) = G(p)I(p), \tag{3}$$

where $p = j\Omega$; Ω is the spatial frequency (line pairs per mm), and $G(p)$ is the transfer function, which can be determined by comparing the measured intensity distributions (see Fig. 6b) and the diffusion approximation [8].

By using the method of transport theory-based finite differences and discrete ordinates [9], we calculated normalised intensity profiles for an infinitely distended slab of 3 cm in thickness. In this case, the optical parameters were varied. The calculated intensity profiles were normalised to their mean value.

The profile of the transmitted photon density of an infinitely distended slab for a point source is proportional to a Gaussian distribution [8]:

$$\Phi(x) \approx y_0 + \frac{A}{w(\pi/2)^{1/2}} \exp\left(-2\frac{x^2}{w^2}\right), \tag{4}$$

where $\Phi(x)$ is the inverse transformation of a delay element of the first order in the system theory. Using the Laplace transformation and the above operator, we obtain the formalised expression for this function [10]

$$F = \frac{1}{1+px}. \tag{5}$$

The values of w and A can be determined for known optical parameters by a linear fit of the calculated profiles by Gaussian distributions.

Using transport theory simulations, we calculated the intensity profiles for a plane-parallel slab by positioning a point light source on one face and calculating the intensity profile on the opposite face.

For a set of stipulated optical parameters (see Table 2), ranging within the healthy and rheumatoid condition of a finger joint, the normalised intensity profiles (normalised to the mean value of all measuring values) were calculated by means of the transport theory. Then, the profiles were fitted by Gaussian distributions. These profiles are shown in Fig. 7a. The parameters of Gaussian distributions (y_0, w, A) were assigned to the optical parameters. A linear fit was used to determine the dependence of the reduced scattering coefficient on the parameter A of Gaussian distributions.

For the constant absorption coefficient $\mu_a = 0.4\ \mathrm{cm}^{-1}$ and anisotropy $g = 0.8$, we obtain $\mu'_s = (2.986A - 3.87)\ \mathrm{cm}^{-1}$. The absorption was kept constant because its influence on the normalised intensity profiles is insignificant.

By means of a linear fit of the reduced scattering coefficient to the parameter A of Gaussian distributions, it was possible to find the linear relation between μ'_s and A (Fig. 7b). All the other optical parameters were kept constant.

Let us return now to the measured intensity profiles presented in Fig. 5. Fig. 8 shows normalised intensity profiles of light scattered by a healthy and rheumatoid fingers. The reduced scattering coefficients were calculated in both cases by the above method. The results are listed in Table 3.

In summary, it can be stated that the method for estimating distributions of light scattered by rheumatoid

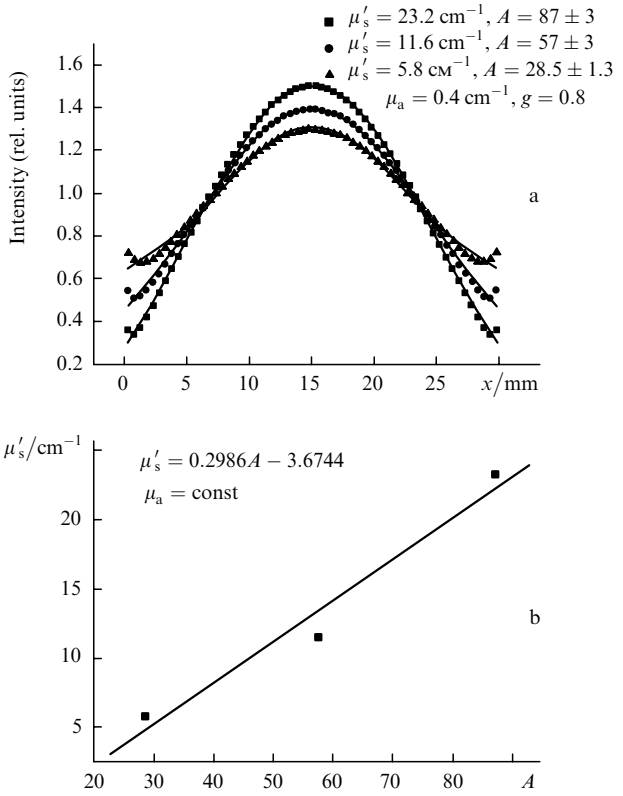

Figure 7. Normalised intensity profiles for a specified set of optical parameters (a) approximated by Gaussian distributions to determine the dependence of the reduced scattering coefficient on the parameter A of the Gaussian distribution, absorption coefficient is $\mu_a = 0.4\ cm^{-1}$ and anisotropy is $g = 0.8$, (b) linear fit of the reduced scattering coefficient as a function of the parameter A of the Gaussian distribution.

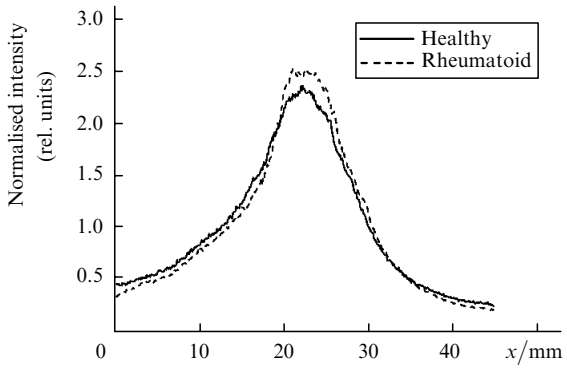

Figure 8. Intensity profiles of rheumatoid and healthy fingers.

finger joints, can be applied as a very rough approximation until a faster algorithm is developed. From the physical point of view, it is obvious that the distribution of scattered light should be the result of one or several convolutions.

Table 3. Assignment of the parameters of the Gaussian distribution to the optical parameters for healthy and rheumatoid fingers.

Condition	Reduced scattering coefficient/cm^{-1}	y_0	w	A
Rheumatoid	26.82	2.71	626.36	766.4
Healthy	10.10	1.77	478	346

3. Validity range of the Gaussian approximation

To check the validity of the Gaussian approximation, it is necessary to solve the radiation transfer equation, without using any physically inadmissible simplifications. For example, the diffusion approximation [8] cannot be used for tissue layers, whose thickness does not considerably exceed the mean free path of photons, or which consist of inhomogeneous structures. The influence of the scattering phase function and reflection at interfaces on the scattered light distribution is another important fact to be considered.

These problems can be solved using the Monte Carlo method. The five-dimensional phase space $\psi = IR^3 \times S^2$ (three-dimensional vector $\boldsymbol{r}$ and two-dimensional vector $\boldsymbol{\Omega}$) is usually sufficient for the description of optics of tissues. For nonstationary cases and consideration of fluorescent radiation, it is extended by the dimensions $IR^+ \times IR^+$ representing energy and time coordinates. The Monte Carlo method is often used for the construction of real images in computer graphics and gives good results in conjunction with advanced technology [11]. Because this method is used to describe scattering of light only from surfaces, it is poorly developed for optics of tissues because in the latter case, scattering occurs in the bulk of the tissue.

Before discussing Monte Carlo simulations with the use of an anatomic model, which is important for tissue optics, we describe a simple heuristic model.

Galton's board (Sir Francis Galton, 1822–1911) (Fig. 9a) proved to be very useful for the investigation of limit theorems in the probability theory. Although the relationship to tissue optics (Fig. 9b) is obvious, relevant applications of this rather simple model have not been discussed so far.

In Galton's board, a large number of identical particles passes through an array of diffusers. While passing through the board, they are deflected to the right with a probability of P and to the left with a probability of $Q = 1 - P$. Therefore, many elementary events (P, Q) take place. A statistically stable distribution over the transverse coordinate x appears for a sufficiently large amount of particles on the bottom of the device. For $P = Q = 1/2$, this distribution is symmetrical with respect to the direction of incidence of particles. This case simulates a homogenous tissue layer, while for the case $P \neq Q$, a predominantly one-directional deflection occurs in the tissue. This is typical for tissues

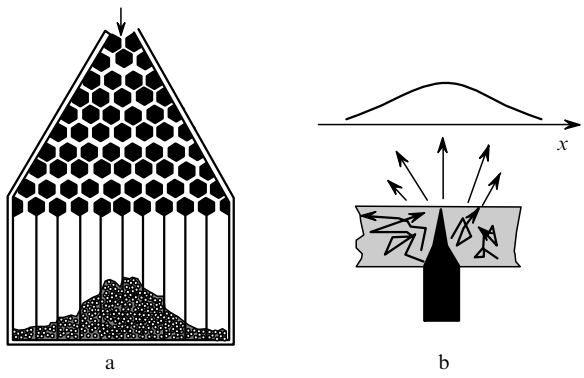

Figure 9. Schematic view of Galton's board (a) and transillumination of a tissue slab (b).

containing asymmetrical structures, such as joints. Within the joint, the photons are partially reflected at the interfaces according to the Fresnel law. In this case, the Gaussian distribution is shifted.

Galton's board demonstrates the law of large numbers. The limiting value of the binomial distribution

$$\lim_{n\to\infty}\binom{n}{k}P^nQ^{n-k}$$

is the Gaussian distribution, with $k \leqslant n$ representing discrete values of x. In our case, it is interesting to consider the correction terms, which appear in the expansion of the Stirling formula into Taylor series in $1/\sqrt{n}$:

$$W=\frac{\exp(-x^2/2)}{(2\pi nPQ)^{1/2}}\left[1+\frac{(x^2-3x)(Q-P)}{6(nPQ)^{1/2}}+O\left(\frac{1}{n}\right)\right], \quad (6)$$

where $|x| = |(k - nP)/(nPQ)^{1/2}|$ is the lateral coordinate.

These terms disappear with increasing n or x, respectively, which means that they are negligible for infinitely extended bodies. For transillumination of finite bodies, however, they are of importance, since the mathematical limiting value $x \to \infty$ also implies an arbitrarily large layer thickness. For thin layers, however, this condition is not fulfilled, which means that the number of elementary events (P, Q) is insufficient to develop a Gaussian distribution. As a consequence, a cut off for small values will occur and the correction terms in (6) result in the asymetric deformation of the Gaussian distribution. Consequently, in the case of an asymmetrical deflection, when $P \neq Q$, the first term of Taylor series is dominant, so that its influence will become noticeable in relatively thick layers. For $P = Q$, however, the limiting Gaussian distribution will be faster approximated by $1/n$, i.e. by the reciprocal value of the layer thickness.

The drawback of this simple model of tissue optics is the lack of backscattering and absorption. Therefore, expression (6) represents an approximation for diffusely forward scattered photons only.

Let us present now the results of Monte Carlo simulations for various tissue-optical situations. We start with relatively thin homogenous tissue layers (Fig. 10), using the optical parameters presented in Section 2. This subject is of essential importance to optical biopsy and optical molecular imaging, especially for rescaling of the detected intensity distribution in the case of fluorescence sources located inside the scattering tissue [12, 13].

The deviation from the Gaussian distribution is particularly strong for collimated irradiation. This effect strongly depends on the dependence of the anisotropy factor g of the scattering phase function on the layer thickness. When such a deviation is investigated, the advantage of the Monte Carlo method becomes apparent. This method also has some advantages in calculations of the radiation distributions in complicated 3D systems.

In our case, this *ab initio* method of the transfer theory is more preferable than deterministic procedures because Monte Carlo algorithms are usually more general. This is the only way to quite exactly describe heterogeneous spatial structures and strongly anisotropic angular distributions of light scattered in tissues.

The calculations performed here were based on the Monte Carlo code AMOS [14, 15], which had been initially

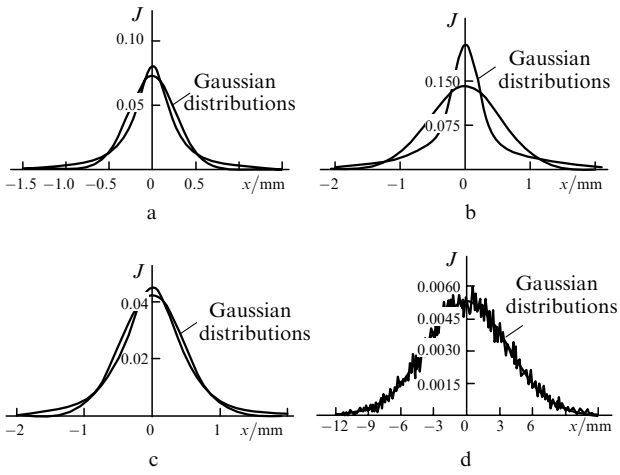

Figure 10. Intensity profiles J for thin homogenous layers: (a) tissue slab 0.2 mm in diameter, diffuse laser illumination; (b) tissue slab 0.2 mm in diameter, collimated laser illumination; (c) tissue slab 0.5 mm in diameter, diffuse laser illumination; (d) tissue slab 30 mm in diameter, collimated laser illumination.

developed to describe the transfer of ionising radiation. At the end of 1990s, this programme was adapted for the description of light propagation, including refraction of light from surfaces. The new code was developed based on the state-of-the-art software technology (OOP and/or OOD) utilising the so-called standard template libraries (STL). Based on the empirical fit of experimentally determined probability density functions, the appropriate distributions of scattered light can be found by using tables.

For a more realistic consideration of small joints, the model shown in Fig. 6a was developed. The model was constructed using intersections and differences of twelve so-called primitive bodies such as cuboids, balls, cylinders and truncated cones. A special attention was devoted to the simulation of the joint cavity and the capsule.

Fig. 11 shows the trajectories of 100 photons and the scattered light distribution for one healthy and one diseased joint. Both the differences between the two conditions and a distinct deviation from the Gaussian shape are visible. One can also clearly see that the distribution of the scattered light in the x direction (transverse direction) is broader than that in the longitudinal direction, which well agrees with the experimental data.

These results can be improved by using a more detailed model providing a higher resolution. The asymmetry has not been included in the diagnostic evaluation so far. The difference images obtained at different wavelengths may also improve diagnostics.

4. Sagittal Optical Tomography

In the assessment of RA stages, a cross-sectional image of the transilluminated plane can be more familiar and helpful for a physician compared to diffuse projections and single figures. An image representing the optical properties in the finger joint requires a reconstruction method. Xu et al. [16] obtained first experimental results on a transversal tomographic imaging of finger joints. Unlike these experiments, we reconstructed the sagittal cross section around the finger joint in the central plane along the finger axis. Hielscher et al. [17] developed algorithms, based on the theory of

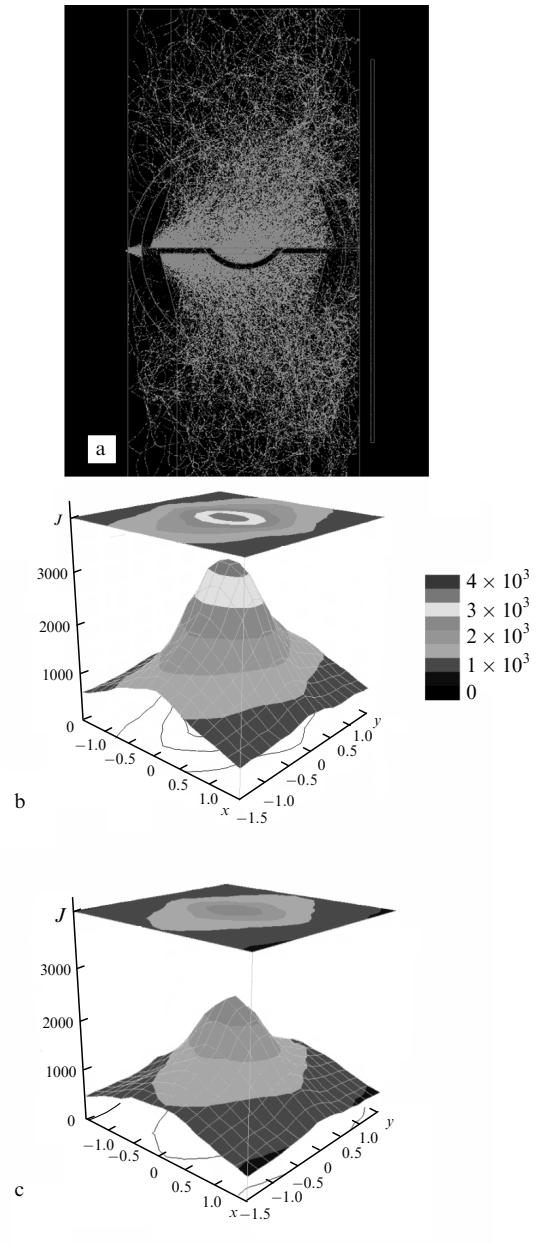

Figure 11. Results of the Monte Carlo simulation: trajectories of 100 photons (a), intensity profiles for a healthy (b), and a rheumatoid small joint (c).

radiation transfer [18], for direct calculations of photon transport in tissues and the iterative reconstruction of distributions of optical parameters in a finger joint. In this section, we describe the simulation of sagittal diffuse optical tomograms of a PIP finger joint in the healthy and early inflammatory states, and consider experimental sagittal optical tomograms.

4.1 Materials and Methods

We discuss the reconstruction of optical parameters in sections of finger joints from sagittal optical tomograms.

First, a numerical model of the finger joint should describe both the anatomical and unknown optical properties of the joint (Fig. 6c). Due to multiple photon scattering in tissues the use of a back-projection algorithm, employed in X-ray tomography for reconstructing the distributions of μ_s and μ_a inside the finger joint is limited. Therefore, a model of the iterative image reconstruction (MOBIIR) should be used [19]. The MOBIIR model consists of two major parts: (1) a forward model for light propagation and (2) an inverse model.

The forward model predicts the readings of a detector located on the tissue surface, when the position of the source and the distribution of optical parameters inside the finger joint are known. The light propagation is mathematically described by the equation of radiation transfer [19]. The detector response at forty positions is calculated for ten positions of the source along the finger. Almost every site in the area between sources and detectors is transilluminated due to the strong scattering of light by human tissue.

Unlike the forward model, the inverse model determines the optical parameters inside tissue by using a given set of calculated and measured detector readings on the tissue surface. The measured detector readings are compared to the predicted detector readings by defining an objective function. The goal is to minimise this objective function to obtain the unknown optical parameters. Thus, the reconstruction process starts with an initial guess of the distribution of the optical parameters inside the tissue. A forward calculation is performed to predict the detector readings and its objective function. The gradient of the objective function leads to a search direction, and a new set of optical parameters is obtained by updating the initial guess. The forward and inverse model are iteratively employed until self-consistency is reached. Once the minimum of the objective function is found, the final set of optical parameters constitutes the tomographic image. The complete reconstruction scheme is described in detail elsewhere [20].

The crucial points of a MOBIIR technique are a physically correct forward algorithm, which describes the photon transport through tissue, an algorithm for the gradient calculation, and an optimisation method to minimise the objective function.

The tomographic imaging of healthy and rheumatoid finger joints was tested by simulation of transillumination. We used the numerical model of the finger joint with both the anatomical and the known optical properties of healthy and rheumatoid joint tissue [4]. The detector readings were generated by the forward model, and with these 'measured' data the inverse reconstruction process was started.

4.2 Results

Fig. 12 shows the sagittal NMR images of two PIP joints of a 60 years old patient for a noninflamed joint (Fig. 12a) and inflammatory RA state (Fig. 12b). The contrast agent in the inflamed joint verifies a physiological RA stage of 2 (Fig. 1). Along with the overall thickening of the finger, the swollen capsule is clearly visible due to increased blood flow in the inflamed synovialis and the diffusion gradient into the affected partial volume.

We found that scattering of light in the joint increased at the first and second stages of the disease. This is confirmed by the results of the optical reconstruction (Fig. 13). The distribution of the reconstructed scattering coefficient μ_s in the transilluminated plane of the model shows an obvious difference between healthy and inflamed state. In the healthy state (Fig. 13a) the joint gap is clearly visible as a low scattering area. Contrary to that, the inflamed state (Fig. 13b) shows high scattering at the location of the joint gap and capsule resp. synovialis. For better understanding,

Figure 12. NMR images of two PIP joints of a 60 years old patient, T1 weighted: (a) no inflammation, no contrast agent; (b) inflammatory RA state with contrast agent (Gadolinium).

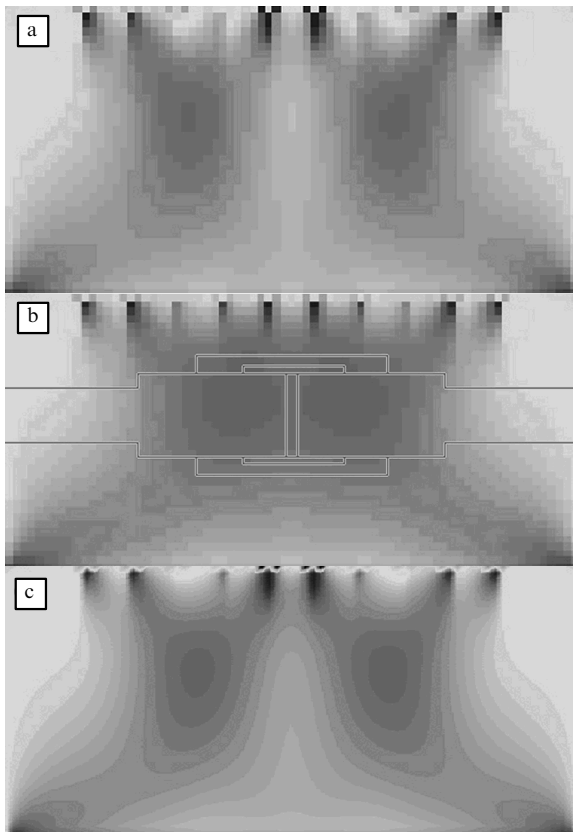

Figure 13. Reconstructed scattering coefficient μ_s in the transilluminated plane of the model: (a) healthy stage; (b) synovialis and synovial fluid with optical properties of inflamed stage; (c) only synovial fluid inflamed, dark areas indicate high scattering, light areas indicate low scattering.

the scheme of the numerical model is superimposed. If only synovial fluid passes from the healthy to the inflamed state (Fig. 13c), the distribution of scattering coefficient is similar to that of the healthy state. This means that upon optical transillumination changes in synovialis are mainly detected rather than changes in the synovia. The decrease in scattering to the left and to the right side is due to the decrease in the number of sources and detectors in this region. Therefore, these outer positions are less transilluminated. This causes a lack of information for exact reconstruction. The highly scattering spots beneath the source and the increase in scattering in the direction of the outer detector positions are artefacts as well. The distribution of absorbers is not shown because its change is negligible.

5. Conclusions

Simulations of sagittal optical tomograms of RA finger joints showed that this imaging method is sensitive to changes in scattering of light in the joint. These changes are more noticeable in the expanded capsule than in the narrow joint gap. In the near future, we will perform clinical tests of the experimental setup to find out if sagittal images of optical properties can safely detect the state of inflammation.

In addition, a new specific fluorescent marker allows a combination of optical tomography with fluorescent imaging techniques. Thus, the simultaneous use of scattering, absorption, and fluorescence will provide the diagnostics of inflamed tissues with an improved resolution and accuracy. We believe that optical tomography can become a useful tool to assist rheumatologists in treatment of RA.

References

1. Beuthan J., Minet O., Müller G., Prapavat V. *SPIE,* **IS 11**, 263 (1993).
2. Steinbrocker O., Traeger C.H., Batermann R.C. *J. Am. Med. Ass.*, **140** (8), 659 (1949).
3. Beuthan J., Prapavat V., Naber R.-D., Minet O., Müller G. *Proc. SPIE Int. Soc. Opt. Ing.*, **2676**, 43 (1996).
4. Beuthan J., Cappius H.-J., Hielscher A., Hopf M., Klose A., Netz U. *Biomedizinische Technik*, **46**, 298 (2001).
5. Scheel A., Krause A., Mesecke-von Rheinbaben I., Metzger G., Rost H., Tresp V., Mayer P., Reuss-Borst M., Müller G.A. *Arthritis Rheum.*, **46** (5), 1177 (2002).
6. Wiener N. *Mathem. Ann.*, **95**, 557 (1926).
7. Kupfmuller K. *Die Systemtheorie der Elektr. Nachrichtenubertragung* (Stuttgart: Hirzel, 1952, 2 Aufl).
8. Arridge S.R., et al. *Phys. Med. Biol.*, **37** (7), 1531 (1992).
9. Klose A.D., Hielscher A.H. *Medical Physics*, **26** (8), 1698 (1999).
10. Philippow E. *Taschenbuch Elektrotechnik* (Berlin: Verlag Technik, 1968) pp 1101 – 1104.
11. Veach E. *PhD Thesis* (Stanford: Department of Computer Science, 1997).
12. Beuthan J., Minet O., Müller G. *IEEE J. of Selected Topics in Quantum Electron.*, **2**, 906 (1996).
13. Minet O., Beuthan J., Licha K., Mahnke C., in *Fluorescence Spectroscopy. Imaging and Probes*. Ed. by R. Kraayenhof, A.J.W.G. Visser, H.C. Gerritsen (Berlin, Heidelberg, NewYork: Springer, 2002) Vol. 2.
14. Henniger J., in *Strahlenschutz: Physik und Messtechnik. Jahrestagung des Fachverbandes fur Strahlenschutz e.V.* (Karlsruhe: Verlag TÜV Rheinland, 1994) Band 1, 26, pp 145 – 150.
15. Minet O., Henniger J., in *Fortschritte in der Lasermedizin 12*. Ed. by H.-P. Berlien, G.A. Müller (Berlin: ecomed, 1995) p. 97.

16. Xu Y., Iftimia N., Jiang H. *J. Biomedical Opt.*, **7** (1), 88 (2002).
17. Hielscher A.H., Klose A.D., Hanson K.M. *IEEE Trans. Med. Imag.*, **18**, 63, 262 (1999).
18. Chandrasekhar S. *Radiative Transfer* (London: Oxford University Press, 1950; New York: Dover Publ. Inc., 1960).
19. Klose A.D., Netz U., Beuthan J., Hielscher A.H. *J. Quant. Spectr. Rad. Transfer*, **72**, (5), 691 (2002).
20. Klose A.D., Hielscher A.H. *J. Quant. Spectr. Rad. Transfer*, **72** (5), 715 (2002).